Pharmacological Research 187 (2023) 106638

Contents lists available at ScienceDirect

Pharmacological Research

journal homepage: www.elsevier.com/locate/yphrs

Anti-inflammatory effects and improved metabolic derangements in *ob/ob* mice by a newly synthesized prenylated benzopyran with pan-PPAR activity

Patrice Marques [a,b,1], Carlos Villarroel-Vicente [a,b,1], Aida Collado [a,b], Ainhoa García [a,b], Laura Vila [b], Isabelle Duplan [c], Nathalie Hennuyer [c], Francisco Garibotto [d], Ricardo D. Enriz [d], Catherine Dacquet [e], Bart Staels [c], Laura Piqueras [a,b,f], Diego Cortes [a,*], María-Jesús Sanz [a,b,f,**], Nuria Cabedo [a,b,*]

[a] *Department of Pharmacology, University of Valencia, Valencia, Spain*
[b] *Institute of Health Research-INCLIVA, University Clinic Hospital of Valencia, Valencia, Spain*
[c] *University of Lille, Inserm, CHU Lille, Institut Pasteur de Lille, U-1011-EGID, F-59000 Lille, France*
[d] *Faculty of Chemistry, Biochemistry and Pharmacy, National University of San Luis-IMIBIO-SL-CONICET, Chacabuco 917-5700, San Luis, Argentina*
[e] *Institut de Recherches Servier, Suresnes 92150, France*
[f] *CIBERDEM-Spanish Biomedical Research Centre in Diabetes and Associated Metabolic Disorders, Carlos III Health Institute, Madrid, Spain*

ARTICLE INFO

Keywords:
Prenylated benzopyran
PPAR
Molecular modeling
Metabolic disorders
Anti-inflammatory effects
ob/ob mice

Chemical compounds studied in this article:
WY-14,643 or Pirinixic acid (PubChem CID: 5694)
GW501516 or Endurobol (PubChem CID: 9803963)
Rosiglitazone (PubChem CID: 77999)

ABSTRACT

Background and purpose: Selective peroxisome proliferator-activated receptors (PPARs) are widely used to treat metabolic complications; however, the limited effect of PPARα agonists on glucose metabolism and the adverse effects associated with selective PPARγ activators have stimulated the development of novel pan-PPAR agonists to treat metabolic disorders. Here, we synthesized a new prenylated benzopyran (BP-2) and evaluated its PPAR-activating properties, anti-inflammatory effects and impact on metabolic derangements.

Experimental approach: BP-**2** was used in transactivation assays to evaluate its agonism to PPARα, PPARβ/δ and PPARγ. A parallel-plate flow chamber was employed to investigate its effect on TNFα-induced leukocyte-endothelium interactions. Flow cytometry and immunofluorescence were used to determine its effects on the expression of endothelial cell adhesion molecules (CAMs) and chemokines and p38-MAPK/NF-κB activation. PPARs/RXRα interactions were determined using a gene silencing approach. Analysis of its impact on metabolic abnormalities and inflammation was performed in *ob/ob* mice.

Key results: BP-**2** displayed strong PPARα activity, with moderate and weak activity against PPARβ/δ and PPARγ, respectively. *In vitro*, BP-**2** reduced TNFα-induced endothelial ICAM-1, VCAM-1 and fractalkine/CX_3CL1 expression, suppressed mononuclear cell arrest via PPARβ/δ-RXRα interactions and decreased p38-MAPK/NF-κB activation. *In vivo*, BP-**2** improved the circulating levels of glucose and triglycerides in *ob/ob* mice, suppressed T-lymphocyte/macrophage infiltration and proinflammatory markers in the liver and white adipose tissue, but increased the expression of the M2-like macrophage marker CD206.

Abbreviations: ALT, alanine aminotransferase; AST, aspartate transaminase; BP-2, benzopyran—2-(ethyl 4'-methylheptenoate)-6-(p-fluorobenzyloxy)-2-(methyl)-benzodihydropyran; BSA, bovine serum albumin; CAM, cell adhesion molecule; CVD, cardiovascular disease; DMSO, dimethylsulfoxide; FFAs, free fatty acids; HDL-c, HDL-cholesterol; HUVEC, human umbilical venous endothelial cells; ICAM-1, intercellular adhesion molecule-1; MCP-1/CCL2, monocyte chemoattractant protein-1; MD, molecular dynamics; MetS, Metabolic syndrome; PPAR, peroxisome proliferator-activated receptor; RXR, 9-cis-retinoic acid receptor; SEM, standard error of the mean; siRNA, small interfering RNA; T2D, type 2 diabetes; TNFα, tumor necrosis factor-α; TZDs, thiazolidinediones/glitazones; VCAM-1, vascular cell adhesion molecule-1; WAT, white adipose tissue.

* Correspondence to: Department of Pharmacology, Faculty of Pharmacy, University of Valencia, Avda Vicente Andres Estelles s/n, 46100 Burjassot, Spain.
** Correspondence to: Department of Pharmacology, Faculty of Medicine, University of Valencia, Avda. Blasco Ibañez 15, 46010 Valencia, Spain.
E-mail addresses: dcortes@uv.es (D. Cortes), maria.j.sanz@uv.es (M.-J. Sanz), ncabedo@uv.es (N. Cabedo).
[1] These authors have equally contributed to this work and share authorship.

https://doi.org/10.1016/j.phrs.2022.106638
Received 14 November 2022; Received in revised form 22 December 2022; Accepted 27 December 2022
Available online 28 December 2022

Conclusion and implications: BP-**2** emerges as a novel pan-PPAR lead candidate to normalize glycemia/triglyceridemia and minimize inflammation in metabolic disorders, likely preventing the development of further cardiovascular complications.

1. Introduction

Metabolic syndrome (MetS) is characterized by the simultaneous occurrence of a cluster of cardiovascular risk factors and has a high prevalence in western countries. MetS is multifactorial and is associated with the development of type 2 diabetes (T2D), cardiovascular disease (CVD) and cancer, among others [1]. There is evidence to support that MetS is linked to low-grade systemic inflammation [2], the main driver of premature atherosclerosis, which, in turn, is the principal contributor to the pathogenesis of myocardial and cerebral ischemic disorders.

Peroxisome proliferator-activated receptors (PPARs) are members of the nuclear hormone receptor superfamily of transcription factors, and are one of the most valuable targets for treating diabetes and hypertriglyceridemia, which are both associated with MetS development [3]. Three isoforms of PPAR [PPARα (NR1C1), PPARβ/δ (NR1C2) 88 and PPARγ (NR1C3)] have been described. Upon activation by endogenous ligands (fatty acids and derivatives) or synthetic agonists (fibrates and thiazolidinediones), PPARs heterodimerize with 9-*cis*-retinoic acid receptors (RXRs) to control the expression of multiple target genes involved in adipogenesis, lipid and glucose metabolism and metabolic homeostasis, as well as cell growth, differentiation and apoptosis [4,5]. The known involvement of PPARs in the control of inflammatory processes has placed them in the spotlight as targets to regulate inflammation, vascular function and vascular remodeling [6]. Notably, PPAR ligands inhibit the activation of inflammatory gene expression and can suppress proinflammatory transcription factor signaling pathways in vascular and inflammatory cells [6,7].

Dual- or pan-PPAR agonists have been demonstrated to be more potent than selective PPAR agonists in correcting both lipid and glucose homeostasis in T2D and MetS [8,9]. Results from clinical trials have, however, revealed important adverse effects caused by PPARγ-selective agonists or dual-PPAR agonists with predominant PPARγ activation that have led to withdrawal of these drugs from the market, or their restricted use. Most of the side effects are, nevertheless, either drug-specific (off-target) or related to excessive PPARγ activation [3,10]. Notably, several studies have found that moderate rather than strong PPARγ activation mitigates its adverse effects and improves its therapeutic profile [10–12].

PPARβ/δ is involved in free fatty acid catabolism and glucose metabolism, and exerts anti-inflammatory effects when activated [4]. While no PPARβ/δ agonists are currently available for clinical use, preclinical studies have proven the beneficial effects of PPARβ/δ activation in hepatic steatosis, obesity, dyslipidemia, T2D, inflammation and leukocyte recruitment [13–15]. Although full PPARβ/δ activation has been associated with carcinogenic and angiogenic properties in rodents [4,5], dual- or pan-PPAR agonists with partial PPARβ/δ and/or PPARγ activation may hold promise as safer therapeutic agents.

Against this background, we recently identified and characterized a potent dual-PPARα/γ agonist—the natural prenylated benzopyran polycerasoidol (BP-1) [16]. BP-1 behaves as a full PPARα and PPARγ activator and exhibits anti-inflammatory activity through inhibition of tumor necrosis factor (TNF)α-induced mononuclear cell-endothelium interactions [16].

In an attempt to find safer and more effective dual PPARα/γ or pan-PPAR agonists, and based on our previous studies with BP-**1** [16], we have synthesized nearly a hundred different compounds. From them, a new prenylated benzopyran—2-(ethyl 4'-methylheptenoate)− 6-(*p*-fluorobenzyloxy)− 2-(methyl)-benzodihydropyran (BP-**2**), displayed in vitro activity on human PPAR (α, β/δ and γ) receptors. Therefore, we also evaluated its potential anti-inflammatory effects on TNFα-induced endothelial dysfunction and the underlying mechanisms involved. Finally, we have investigated its effectiveness in vivo in improving cardiometabolic derangement in obese/diabetic mice.

2. Materials and methods

2.1. Chemistry

All the details related to the synthesis of BP-**2** are described in the Supplementary file.

2.2. In vitro experiments

2.2.1. Transactivation assays

PPAR transcriptional activity was monitored using a human chimera PPAR/Gal4 gene reporter luciferase system with COS-7 cells (CRL-1651, ATCC, Manassas,VA). The response to BP-**2** was compared with the following positive controls: WY-14,643 (PubChem CID: 5694) for PPARα; GW501516 (PubChem CID: 9803963) for PPARβ/δ; and rosiglitazone (PubChem CID: 77999) for PPARγ (Sigma-Aldrich). The EC_{50} was determined using a concentration range from 0.001 to 10 μmol/L. Luciferase activity was normalized to internal control β-galactosidase activity. Further details can be found in the Supplementary file.

2.2.2. Cell culture studies

All research with human samples in this study complied with the principles of the Declaration of Helsinki and also those approved (No. 2018/076) by the Institutional Ethics Committee of the University Clinic Hospital of Valencia (Valencia, Spain). Written informed consent was obtained from all volunteers.

Human mononuclear cells and neutrophils were obtained from buffy coats of healthy donors, as described [17]. Human umbilical venous endothelial cells (HUVEC) were isolated by collagenase treatment [18]. Prior to every experiment, HUVEC were incubated for 24 or 48 h in medium containing 0.1 or 1% fetal bovine serum, according to the experimental protocol. Further details can be found in the Supplementary file.

2.2.3. Cytotoxicity studies

The cytotoxicity of BP-**2** was assessed on neutrophils and HUVEC at 10, 30 and 100 μmol/L by flow cytometry to assess apoptosis and survival [19], using the FITC Annexin V Apoptosis Detection Kit I (BD Biosciences, San Jose, CA), as described [20]. Further details can be found in the Supplementary file.

2.2.4. RXRα, PPARα and PPARβ/δ silencing via small interfering RNA

Confluent HUVEC were transfected with either a control small interfering RNA (siRNA) or with RXRα-, PPARα- or PPARβ/δ-specific siRNAs (50 nM; GE Healthcare Dharmacon, Inc., Lafayette, CO) using Lipofectamine RNAiMAX (Invitrogen, Carlsbad, CA) for 48 h. Western blotting was used to confirm the silencing efficiency. Further details can be found in the Supplementary file.

2.2.5. Leukocyte-HUVEC interactions under flow conditions

Confluent HUVEC were incubated with vehicle – 0.1% dimethylsulfoxide (DMSO) – or stimulated with TNFα (20 ng/mL, Sigma-Aldrich) for 24 h. BP-**2** (0.1–100 μmol/L) or vehicle were added to plates 24 h prior to TNFα stimulation. Freshly isolated human neutrophils or mononuclear cells were then perfused across the endothelial monolayer as described [21]. Cell adhesion on the surface of the

endothelium was visualized and recorded using an inverted microscope (Axio Observer A1, ZEISS International, Oberkochen, Germany).

Next, to investigate the possible involvement of RXRα, PPARα or PPARβ/δ in the BP-**2**-mediated inhibition of TNFα-induced mononuclear cell adhesion, confluent HUVEC were transfected with either control, RXRα-, PPARα- or PPARβ/δ-specific siRNAs for 48 h. Cells were then pretreated for 24 h with vehicle (0.1% DMSO), BP-**2** (3 μmol/L), WY-14,643 (3 μmol/L) or (GW501516, 1 μmol/L) before stimulation for 24 h with TNFα (20 ng/mL, Sigma-Aldrich), and mononuclear cell-endothelial cell interactions determined [21]. Further details can be found in the Supplementary file.

2.2.6. Determination of endothelial cell adhesion molecule (ICAM-1 and VCAM-1) and fractalkine (CX_3CL1) expression

The expression of intercellular adhesion molecule-1 (ICAM-1), vascular cell adhesion molecule-1 (VCAM-1), and the membrane-bound form of fractalkine (CX_3CL1) on HUVEC was analyzed by flow cytometry. Cells were pretreated for 24 h with BP-**2** (3 μmol/L) or vehicle (0.1% DMSO) and then stimulated for 24 h with TNFα (20 ng/mL). After detachment, HUVEC were incubated with fluorochrome-conjugated antibodies against human ICAM-1, VCAM-1 or CX_3CL1 (1:10 dilution). Cells were then analyzed by flow cytometry and results are presented as the mean fluorescence intensity. Further details can be found in the Supplementary file.

2.2.7. Immunofluorescence

HUVEC were grown to confluence on glass coverslips. In some experiments, cells were treated for 24 h with BP-**2** (3 μmol/L) or vehicle (0.1% DMSO) and stimulated for a further 24 h with TNFα (20 ng/mL). Next, cells were washed, fixed, blocked and then incubated with a primary antibodies against human ICAM-1, VCAM-1 or a fractalkine/CX_3CL1 (1:200 dilution, Abcam, Cambridge, UK), and then incubated with a secondary Alexa Fluor 488-conjugated antibody (1:500 dilution, Invitrogen, Life Technologies, Carlsbad, CA). Cell nuclei were counterstained with Hoechst dye and images were captured with a fluorescence microscope (Axio Observer A1, ZEISS International, Oberkochen, Germany). Further details can be found in the Supplementary file.

2.2.8. Quantification of soluble chemokines in cell supernatants

Human soluble fractalkine/CX_3CL1 and monocyte chemoattractant protein-1 (MCP-1/CCL2) were determined in the supernatant of HUVEC by specific ELISA (R&D Systems, Inc., Minneapolis, MN). Results are presented as ng/mL or pg/mL of chemokine in the supernatant. Further details can be found in the Supplementary file.

2.2.9. Flow cytometry analysis of activated p38-MAPK and NF-κB

The effect of BP-**2** on TNFα-induced p38-MAPK and NF-κB activation was determined in HUVEC by flow cytometry, as described [22]. HUVEC were incubated for 24 h with BP-**2** (3 μmol/L) or vehicle (0.1% DMSO) and then stimulated for 1 h with TNFα 20 ng/mL. Detached cells were fixed and permeabilized, and then incubated with saturated amounts of fluorochrome-conjugated antibodies against human p38 MAPK or NF-κB p65. Samples were run in a flow cytometer and results are presented as the mean fluorescence intensity. Further details can be found in the Supplementary file.

2.3. In vivo experiments

Animal studies were carried out in compliance with the ARRIVE 2.0-Guidelines [23] and in accordance with the EU Directive 2010/63/EU for animal experiments. Animal handling and experimental protocols were approved by the Animal Experimentation Ethics Committee of the University of Valencia (Protocol No. A1469445706311). Six-week-old male *ob/ob* mice (C57BL/6. Cg-Lep^{ob}/J) were supplied by Charles River Laboratories International (Wilmington, MA).

Blood samples of 6 h-fasted mice were collected for glucose baseline measurement. Mice, randomly divided into three groups ($n = 7$ per group), were daily treated with vehicle (1% hydroxyethyl cellulose, Sigma-Aldrich) or with BP-**2** at 10 mg/kg or 30 mg/kg, for 15 days by oral gavage. The doses of BP-**2** were selected based on the results obtained in the transactivation assays, previously reported effects of new PPAR agonists or standard reference compounds on adipogenesis, lipid and glucose metabolism in *ob/ob* mice [24–27]. After 15 days of treatment, mice were anaesthetized by isoflurane inhalation and blood samples were collected into heparin or EDTA-containing tubes by cardiac puncture. Plasma samples were obtained and stored at − 80 ºC. Liver and epididymal white adipose tissue (WAT) were extracted and part of both organs were quickly frozen in liquid N_2 for qPCR studies (see *2.3.3. Determination of mRNA expression by quantitative RT-PCR*), and the remainder was OCT embedded for cryosectioning and immunofluorescence studies (see *2.3.2. Histological and immunohistochemical analysis*). Further details can be found in the Supplementary file.

2.3.1. Flow cytometry studies

Saturated amounts of fluorochrome-conjugated monoclonal antibodies were added to blood samples. After 30 min-incubation, erythrocytes were lysed using a commercial buffer, and samples were run in a BD LSRFortessa™ X-20 flow cytometer (BD Biosciences). The gating strategy (Fig. S6), as well as all the material used, including the fluorochrome-conjugated antibodies, are described in the Supplementary file.

2.3.2. Histological and immunohistochemical analysis

Epididymal WAT obtained from the epididymis (visceral fat) and liver samples were embedded in OCT (SLEE medical GmbH, Mainz, Germany), rapidly frozen in liquid N_2, cryosectioned with a cryostat microtome (MNT, SLEE medical GmbH), and mounted on microscope slides (Trajan Serie 3 Adhesive; Trajan Scientific and Medical, Ringwood, Australia).

After fixation and blockage, WAT and liver cross-sections were incubated with primary antibodies against mouse CD3 or F4/80 (1:100 dilution, Abcam) to quantify T-lymphocyte or macrophage infiltration, respectively. Samples were then stained with Alexa Fluor 488-conjugated antibodies (1:1000 dilution, Invitrogen, Life Technologies), while cell nuclei were counterstained with Hoechst dye. Fields from each section were captured (Axio Observer A1 inverted microscope, ZEISS International, Oberkochen, Germany), digitized, and analyzed (ImageJ software 1.48 V, Bethesda, MA). Further details can be found in the Supplementary file.

2.3.3. Determination of mRNA expression by quantitative RT-PCR

Total RNA from murine WAT and liver samples was extracted and purified by standard methods. cDNA was amplified with specific primers for mouse *Tnfα*, *Mcp-1/Ccl2*, *Cx$_3$cl1*, *Cd206*, *Cpt1a*, *Pdk4* or *Apoc3* using a QuantStudio 5 Real-Time PCR (RT-PCR) System and Universal Master Mix (All purchased from Applied Biosystems). Relative quantification of the different transcripts was determined by the $2^{-\Delta\Delta Ct}$ method with *Gapdh* as an endogenous control and normalized to the vehicle group. Further details can be found in the Supplementary file.

2.3.4. Biochemical assessment

Levels of total cholesterol, HDL-cholesterol (HDL-c), triglycerides, alanine aminotransferase (ALT), aspartate transaminase (AST) and free fatty acids (FFAs) were determined using commercial kits, while non-HDL cholesterol was calculated (total cholesterol - HDL-c). Glucose levels were determined using a glucometer, while insulin and adiponectin levels were measured by ELISA assay. The HOMA-IR index was calculated (fasting blood glucose × fasting plasma insulin/22.5) [28]. Liver triglyceride content was determined by enzymatic measurement of glycerol content [29]. All material and further details can be found in the Supplementary file.

2.3.5. Determination of plasma levels of cytokines and chemokines

Murine TNFα, MCP-1/CCL2 and fractalkine/CX_3CL1 plasma levels were measured by ELISA (R&D Systems, Abingdon, UK). Results are expressed as pg/mL or ng/mL of cytokine or chemokine in plasma. Further details can be found in the Supplementary file.

2.4. Statistical analysis

All data are presented as mean ± standard error of the mean (SEM), and analysis was performed using GraphPad Prism 6.0 software (GraphPad Software, Inc., La Jolla, CA). Differences between two groups were determined using an unpaired Student's t-test (parametric analysis) in data that passed both normality (Kolmogorov-Smirnov test) and equal variance (Levene test); otherwise, the non-parametric Mann-Whitney U-test was performed. Differences between multiple groups were analyzed by one-way analysis of variance (ANOVA) with Bonferroni's post hoc analysis in data that passed both normality and equal variance; otherwise, the non-parametric Kruskal-Wallis test followed by Dunn's post hoc analysis was used. Data were considered statistically significant when the *P* value was < 0.05. From previous experience with this murine model along with a priori power analysis, we determined that a sample size of 7 mice per group would be sufficient to evaluate the effects of BP-**2** on biochemical parameters.

3. Results

3.1. Synthesis of BP-2

The 2-(ethyl 4'-methylheptenoate)− 6-(*p*-fluorobenzyloxy)− 2-(methyl)-benzodihydropyran (BP-**2**) (Fig. 1), a polycerasoidol (BP-**1**) analog, was efficiently synthesized in six steps (Fig. S1). Molecular modeling studies showed that the phenolic and the carboxylic group of BP-**2** function as anchoring points on the PPARα, PPARβ/δ or PPARγ binding pocket. A detailed description of the synthetic approach, characterization of compounds and molecular modeling studies is provided in the Supplementary file.

3.2. BP-2 exhibits pan-PPAR agonism

BP-**2** was assayed in vitro for PPARα, PPARβ/δ and PPARγ transactivation activity, using WY-14,643, GW501516 and rosiglitazone as reference compounds for hPPARα, hPPARβ/δ and hPPARγ transactivation, respectively. Used at 10 μmol/L, BP-**2** showed full agonism for hPPARα, partial agonism for hPPARβ/δ and weak agonism for hPPARγ. EC_{50} values revealed potencies in the low micromolar range. By contrast, the natural compound polycerasoidol (BP-**1**) displayed dual full PPARα/γ agonism, with EC_{50} values within the nanomolar range (Table 1).

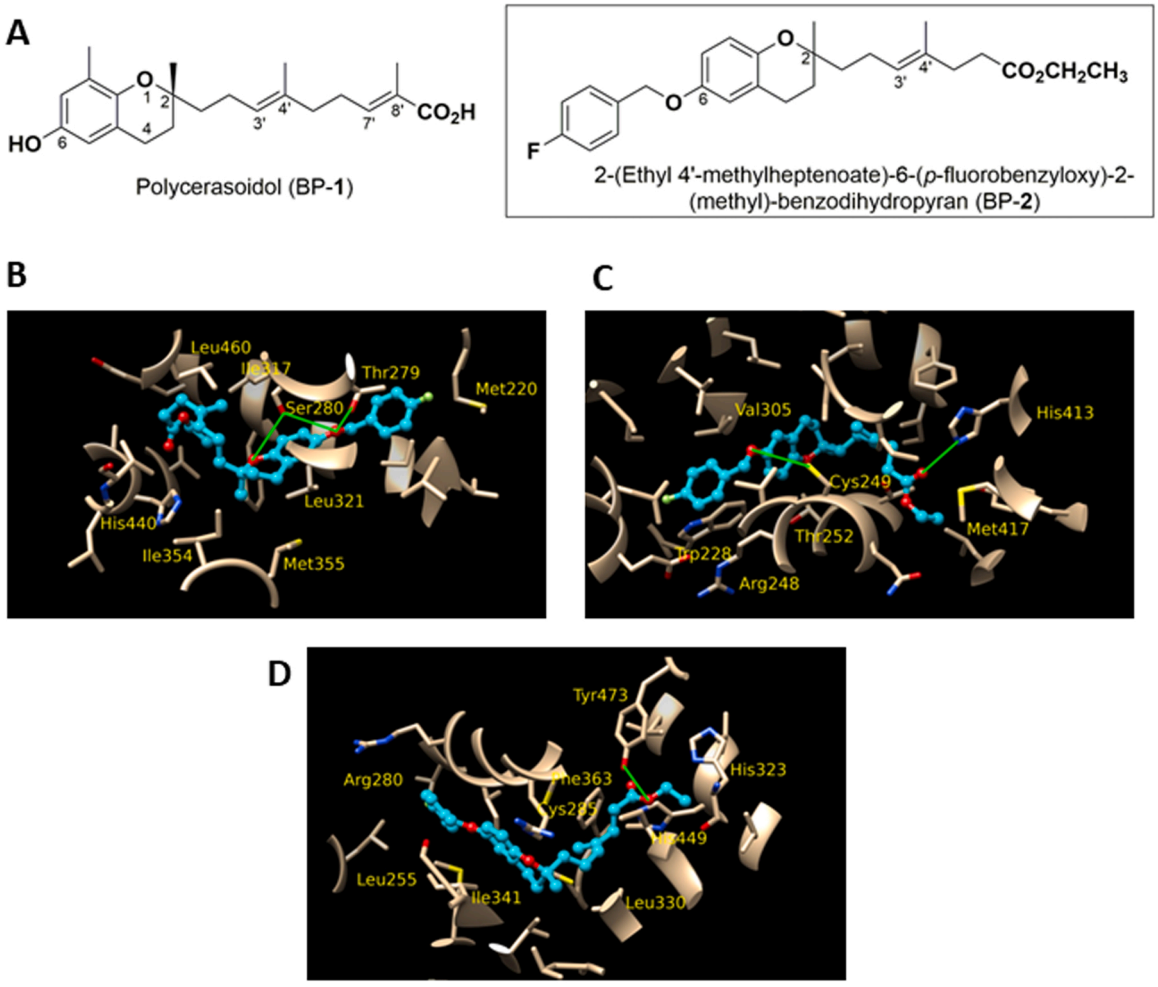

Fig. 1. Chemical structure of BP-2, its analog (polycerasoidol, BP-1), and spatial view of its interaction with PPARs using docking studies. Bioactive prenylated benzopyrans (A). Spatial view of synthetic BP-2 (blue)/PPARα interaction (B), BP-2/PPARβ/δ (C) and BP-2/PPARγ interaction (D). The names of the residues involved in the main interactions are shown in the figure.

Table 1
Evaluation of agonist activity in a cell-based transactivation assays for human PPAR/Gal_4 receptors. EC_{50} values against human PPARα/Gal_4, PPARβ/δ/Gal_4 and PPARγ/Gal_4 receptors.

	Efficacy (%) at 10 μmol/L			EC_{50} (nmol/L)		
	PPARα	PPARβ/δ	PPARγ	PPARα	PPARβ/δ	PPARγ
Polycerasoidol (BP-**1**)	107	NA†	95	184	NA	84
BP-**2**	173	58	26	1294	1718	2480
WY-14,643	100	NA†	NA†	4193	NA†	NA†
GW501516	NA†	100	NA†	NA†	894	NA†
Rosiglitazone	NA†	NA†	100	NA†	NA	60

Note. Efficacy: Emax was the maximal PPAR fold-activation relative to maximum activation obtained with WY14,643 (10 μmol/L), GW501516 (1 μmol/L) and rosiglitazone (1 μmol/L) corresponded to 100% in GAL4 chimeric hPPARα, hPPARβ/δ and hPPARγ system. NA: not active.

3.3. Molecular modeling studies

PPARs have multiple binding points to accommodate a wide range of structural ligands owing to their multiple binding points [30]. The complexes ligand/PPARα, ligand/PPARβ/δ and ligand/PPARγ were model-built and molecular dynamics (MD) simulations were performed for BP-**2**, WY-14,643, GW501516 and rosiglitazone. Docking analysis localized BP-**2** in the binding pocket (Figs. 1B–D and S2), and MD simulations determined the molecular interactions between BP-2, WY-14,643, GW501516 and rosiglitazone with PPARα, PPARβ/δ and/or PPARγ. In addition, the MM-GSA free energy decomposition indicated the residues of the active site in PPARα, PPARβ/δ and PPARγ (Fig. S3). The spatial view of the complex of BP-2 with PPARα in the binding pocket is depicted in Figs. 1B and S2A. Simulations obtained for the complex showed the relevance of His440, Leu321, and Ser280 for ligand binding, which is in agreement with those obtained for WY-14,643 [16]. Other residues making significant interactions to stabilize this complex were Cys276, Thr279, Met355 and Ile354 (Fig. S3A). While WY-14,643 showed a stronger interaction with Lys358 (5.4 kcal/mol) than BP-2 (1 kcal/mol), BP-2 established a stronger interaction with Ile354 and Met355 than WY-14,643 (Fig. S3A). Nevertheless, the simulations indicated that the spatial ordering adopted by BP-2 is quite similar to that of WY-14,643. Simulations obtained for the complex of BP-2 with PPARβ/δ in the binding pocket highlighted the relevance of Arg248, Cys249, Thr253, Ile327 and His413 for ligand binding (Figs. 1C, S2B and S3B), which accords with those reported previously for GW501516 [31]. Other residues making significant interactions to stabilize this complex were Trp228, Val245, Thr252, Ile290 and Val305 (Figs. S2B and S3B). The interaction energy histogram obtained for GW501516 was closely related to that obtained for BP-2 (Fig. S3B); however, GW501516 had a stronger interaction with His287 and Tyr437 (−6.86 and −6.93 kcal/mol, respectively) than BP-2 (−0.4 and −0.7 kcal/mol, respectively). Additionally, the interactions of GW501516 with Val305 (−2.9 kcal/mol) and His413 (−7.3 kcal/mol) were also markedly stronger than those exerted by BP-2 (−1.7 and −2.5 kcal/mol, respectively). These results suggest that GW501516 has a higher affinity for PPARβ/δ than does BP-2. Finally, the spatial view of BP-2/PPARγ complex in the binding pocket is depicted in Figs. 1D and S2C. MD simulations indicated the relevance of Cys285, Arg280, Arg288, Leu330, Ile341, and His449 for ligand binding. The spatial ordering adopted by BP-**2** was quite similar to that obtained for rosiglitazone (Fig. S2C).

3.4. BP-2 is not cytotoxic to human neutrophils and HUVEC at the concentrations tested

BP-**2** was tested at 10, 30 and 100 μmol/L (approximately 10-, 30- and 100-fold higher than the EC_{50} for PPARα agonism, respectively) to evaluate its potential cytotoxic effects in freshly isolated human neutrophils and primary cultures of HUVEC. No cytotoxic effects were observed at any of the tested concentrations (Fig. S4).

3.5. BP-2 inhibits mononuclear cell adhesion to TNFα-stimulated endothelial cells through the down-regulation of ICAM-1, VCAM-1 and fractalkine/CX_3CL1 expression and through the inactivation of p38 MAPK/NF-κB

Whereas BP-**2** treatment of HUVEC at a concentration of 3 or 100 μmol/L had no effect on TNFα-induced neutrophil-HUVEC interactions (Fig. 2A), it significantly inhibited mononuclear cell adhesion to HUVEC at 3 μmol/L (Fig. 2B), and this inhibition was concentration-dependent (Fig. 2C). The IC_{50} for BP-**2** was 0.47 μmol/L, which is ~2 and ~10-fold less than the IC_{50} for rosiglitazone and the natural polycerasoidol BP-**1** (1.1 and 4.9 μmol/L, respectively) [16].

This finding prompted us to examine the effect of BP-**2** on the expression of relevant CAMs (ICAM-1 and VCAM-1) and the membrane-bound form of fractalkine/CX_3CL1. As expected, TNFα stimulation increased ICAM-1, VCAM-1 and fractalkine/CX_3CL1 expression on HUVEC, as revealed by flow cytometry analysis (Fig. 3A–C). Notably, BP-2 treatment diminished the TNFα-induced expression of ICAM-1 by 20.5% (Fig. 3A), VCAM-1 by 26.9% (Fig. 3B) and fractalkine/CX_3CL1 by 42.5% (Fig. 3C). These findings were confirmed by immunofluorescence (Fig. 3E). Moreover, TNFα stimulation of HUVEC led to the generation and release of soluble fractalkine/CX_3CL1 and MCP-1/CCL2 (Fig. 3D and F). While BP-2 treatment significantly lowered the levels of soluble fractalkine/CX_3CL1 induced by TNFα by 70.3% (Fig. 3D), it had no effect on MCP-1/CCL2 levels (Fig. 3F).

Accumulating data indicate that MAPK signaling pathways are modulated by PPAR ligands [22,32]. To investigate the intracellular signaling pathways underlying the inhibitory responses induced of BP-**2**, HUVEC were stimulated with TNFα for 1 h in the presence or absence of BP-**2** (3 μmol/L, 24 h) before pathway analysis. Results showed that BP-**2** significantly blunted the TNFα-induced phosphorylation of p38-MAPK by 59.3% (Fig. 3G). Activation of MAPK family components is associated with the transactivation of NF-κB [33], and its translocation into the nucleus activates the transcription of genes controlling endothelial cell adhesion molecules (CAMs) expression and chemokine synthesis [34]. Notably, BP-2 inhibited the activation of NF-κB induced by TNFα by 60% (Fig. 3H).

3.6. BP-2-inhibited mononuclear cell adhesion to dysfunctional endothelium is partly governed by RXRα-PPARβ/δ interactions

Upon ligand binding, PPARs form heterodimers with the 9-*cis* retinoic acid receptor (RXRα) and bind to specific DNA regions to regulate transcription of genes containing PPAR response elements [21]. As BP-**2** is a pan-PPAR ligand with weak PPARγ activity, we individually knocked down the expression of RXRα, PPARα and PPARβ/δ in endothelial cells using an siRNA approach to test their contribution to BP-**2** inhibitory effect. Western blotting analysis showed that protein expression of RXRα, PPARα and PPARβ/δ in HUVEC was decreased by 49.3%, 57.8% and 46.6%, respectively, confirming the silencing efficiency (Fig. S5). TNFα stimulation of control siRNA-transfected cells triggered a significant increase in mononuclear cell arrest, which was inhibited by BP-**2** (3 μmol/L) or GW501516 (1 μmol/L) by 63.4% and 46.1% respectively, but not by WY-14,643 (3 μmol/L) (Fig. 4A–C). Of note, the BP-2-related responses of mononuclear cells were abolished in HUVEC silenced for RXRα (Fig. 4A) and PPARβ/δ (Fig. 4C) expression, but not in cells silenced for PPARα (Fig. 4B). Additionally, to further asses the siRNA results, we determined the inhibitory effect of BP-2 on TNF-α-induced mononuclear cell arrest in the presence of a specific PPARα (GW6471) or PPARβ/δ (GSK0660) antagonist (Fig. 4D). This inhibitory effect was completely abolished when BP-**2** was incubated in the presence of the PPARβ/δ antagonist (GSK0660) but not with the PPARα antagonist (GW6471).

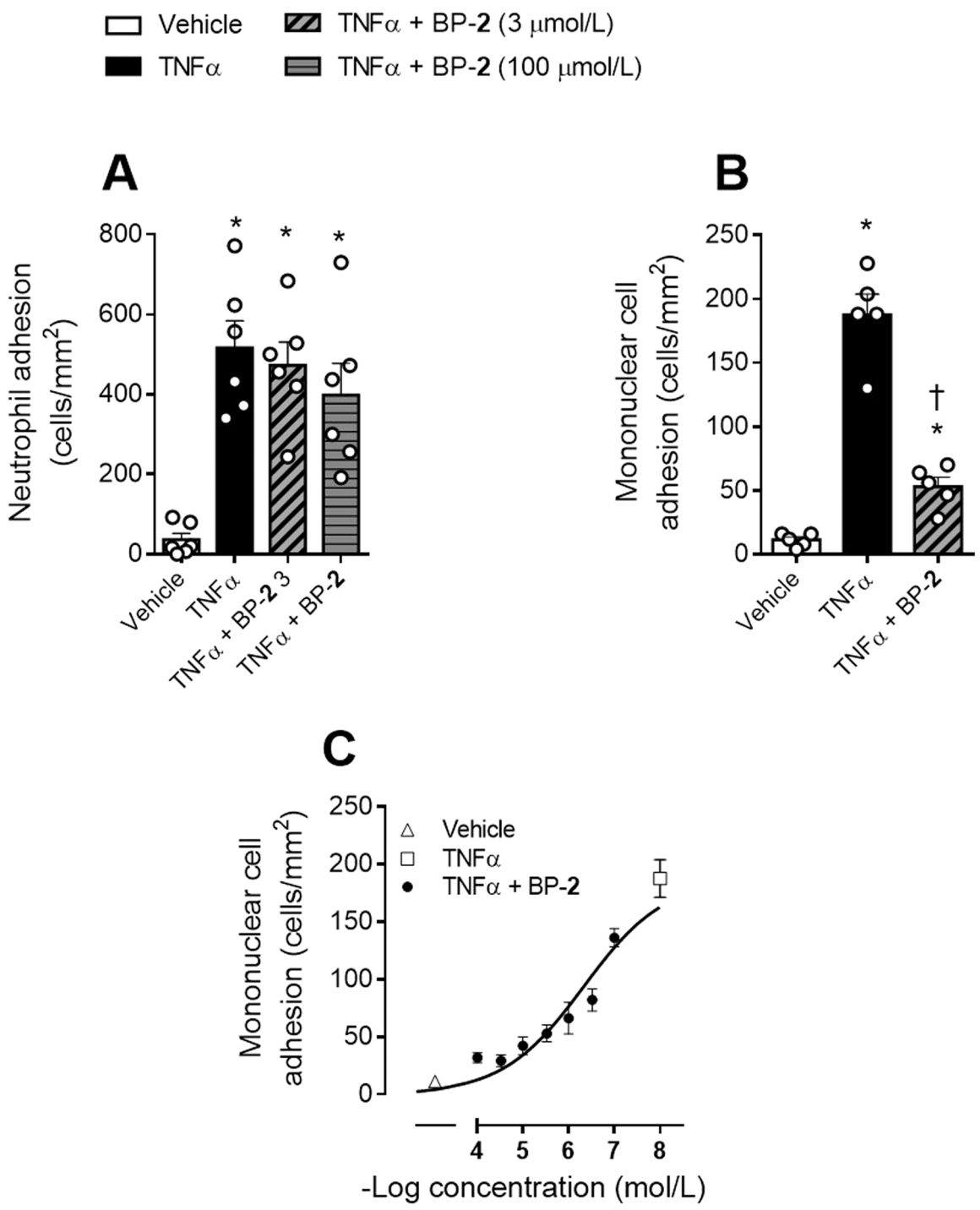

Fig. 2. BP-2 inhibits TNFα-induced mononuclear cell adhesion to HUVEC under physiological flow in a concentration-dependent manner. Cells were pretreated for 24 h with BP-2 or vehicle, prior to TNFα stimulation (20 ng/mL, 24 h), and freshly isolated human neutrophils or mononuclear cells were perfused across the endothelial monolayers for 5 min at 0.5 dyn/cm^2. Neutrophil adhesion was quantified when HUVEC were pretreated with BP-2 at 3 and 100 μmol/L (A); mononuclear cell adhesion was quantified when HUVEC were pretreated with BP-2 at 3 μmol/L (B); concentration-response curve for BP-2 at a concentration range from 0.1 to 100 μmol/L (C). Results are expressed as number of adhered cells/mm^2. Values are presented as mean ± SEM of 5–6 independent experiments. * $P < 0.05$ relative to the vehicle, $^{\dagger}P < 0.05$ relative to the TNFα-stimulated cells.

3.7. BP-2 improves blood glucose and triglyceride levels in ob/ob mice

Full PPARγ agonism effects such as those exerted by glitazones (TZDs), are associated with numerous adverse events, including body-weight gain, in both animal models and humans [4,35]. *In vivo* administration of BP-**2** in *ob/ob* mice at 10 or 30 mg/kg/d did not provoke body-weight gain or variations in food intake (Table 2), but significantly improved glycemia ($\bar{x}$ = 43.7% reduction vs. vehicle) and triglyceride levels ($\bar{x}$ = 68.8% reduction vs. vehicle) at both doses tested (Table 2). However, no significant differences were observed in HOMA-IR index, or in circulating levels of insulin, adiponectin, total cholesterol, HDL-c, non-HDL-c or FFAs (Table 2).

Analysis of common liver injury markers [36] revealed that BP-**2** treatment significantly diminished (at both tested doses) the activity of

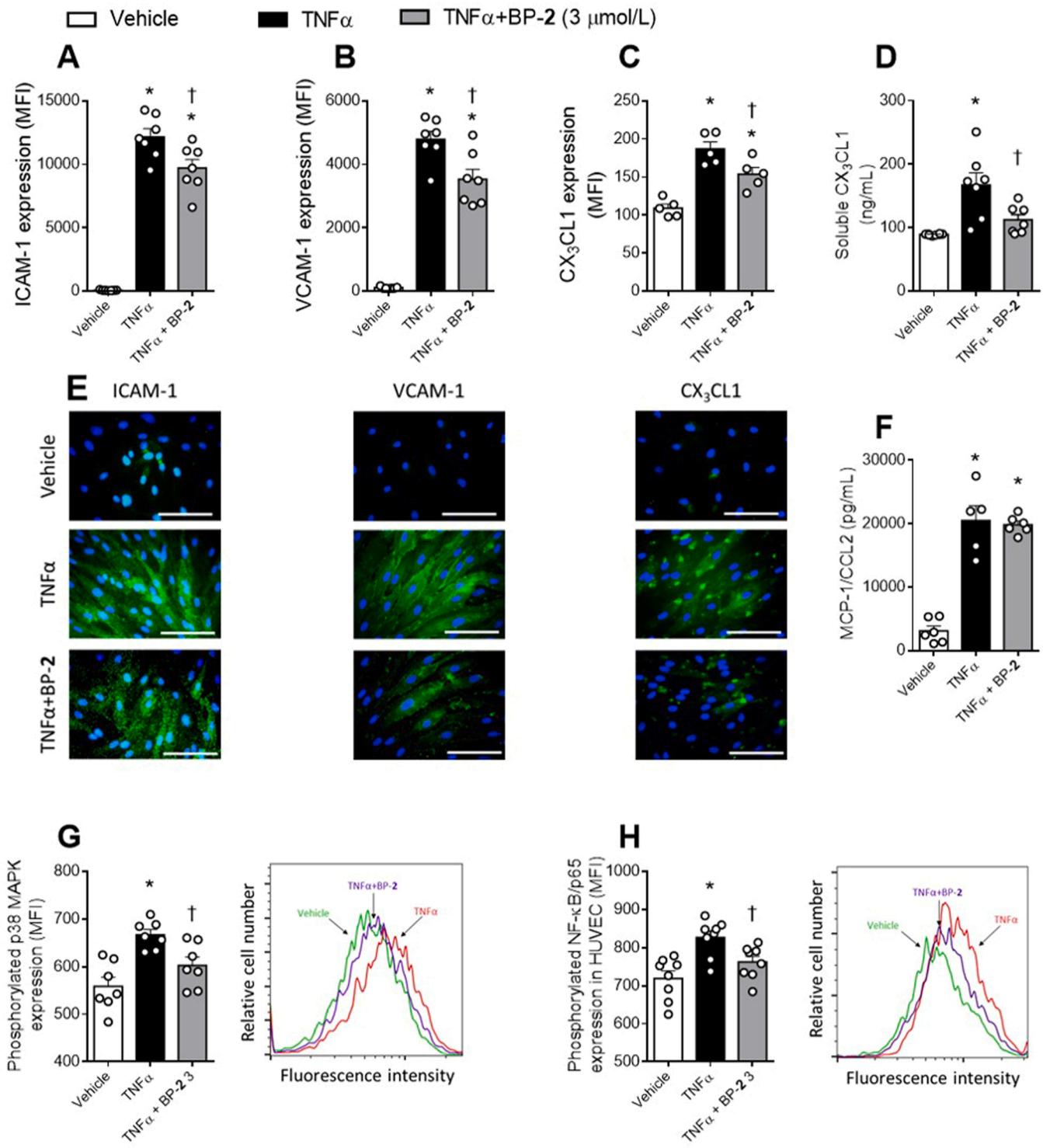

Fig. 3. BP-2 suppresses TNFα-induced ICAM-1, VCAM-1 and transmembrane fractalkine/CX_3CL1 expression, p38 MAPK/NF-κB activation and the release of soluble fractalkine/CX_3CL1 in HUVEC. Cells were pretreated with BP-2 (3 μmol/L) or vehicle for 24 h before TNFα stimulation (20 ng/mL, 24 h for A–F or 1 h for G and H). Results are expressed as mean fluorescence intensity (MFI) of ICAM-1 (A), VCAM-1 (B) and transmembrane fractalkine/CX_3CL1 (C) on HUVEC. Concentration of soluble CX_3CL1 (D) or monocyte chemoattractant protein-1 (MCP-1/CCL2, F) is expressed as ng/mL or pg/mL, respectively. Phospho-p38 MAPK (G) or phospho-NF-κB/p65 (H) are expressed as mean fluorescence intensity (MFI) and representative histograms are also shown. Values are presented as mean ± SEM of 5–7 independent experiments. * $P < 0.05$ relative to the vehicle, † $P < 0.05$ relative to the TNFα-stimulated cells. ICAM-1, VCAM-1 and transmembrane CX_3CL1 expression were also visualized on HUVEC by immunofluorescence using primary rabbit antibodies against ICAM-1, VCAM-1 or fractalkine/CX_3CL1 and an secondary Alexa Fluor 488-conjugated goat anti-rabbit antibody (green). Cell nuclei were counterstained with Hoechst (blue) (E). Scale bar = 100 μm.

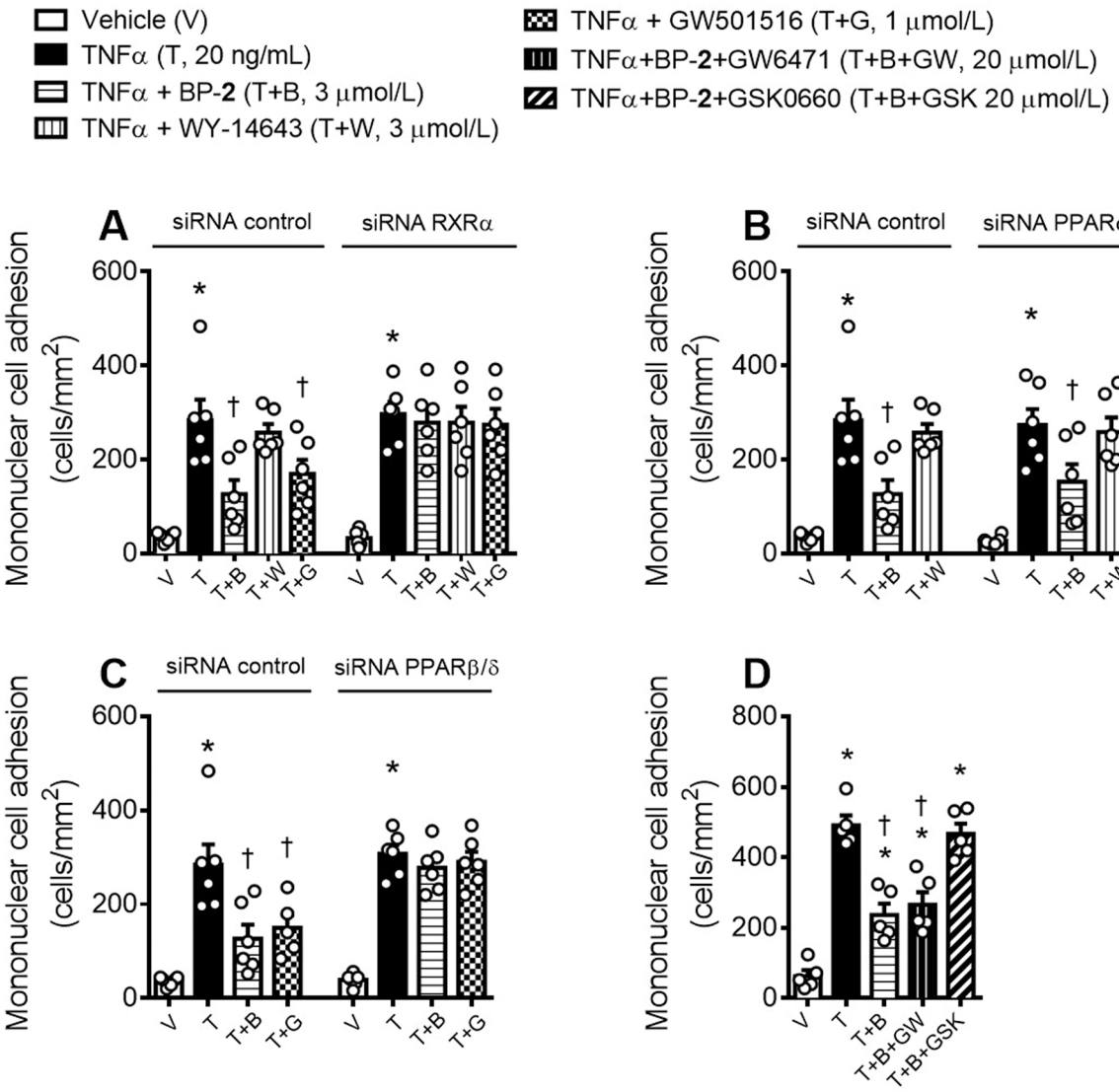

Fig. 4. Silencing of RXRα or PPARβ/δ, but not PPARα, abolishes the inhibitory effect of BP-2 on TNFα-induced mononuclear leukocyte-endothelial cell interactions. HUVEC were transfected with control and RXRα- (A), PPARα- (B) or PPARβ/δ-specific (C) siRNAs. At 48 h after transfection, cells were pretreated with BP-2 (3 μmol/L), WY-14,643 (3 μmol/L), GW501516 (1 μmol/L) or vehicle for 24 h and then stimulated for a further 24 h with TNFα (20 ng/mL). Additionally, some HUVEC were incubated with a PPARα- (GW6471, 20 μmol/L) or a PPARβ/δ-antagonist (GSK0660, 20 μmol/L). Four hours later, some plates were treated with BP-2 for 24 h and then incubated with vehicle or stimulated with TNFα for another 24 h (D). Mononuclear cell adhesion was then quantified. Values are presented as mean ± SEM of 5–6 independent experiments. * $P < 0.05$ relative to the respective vehicle group, † $P < 0.05$ relative to the respective TNFα-stimulated cells.

ALT and AST by 43.8% and 43.7%, respectively (at 10 mg/kg/d), when compared with the activity in vehicle-administered mice (Table 2).

3.8. BP-2 lowers the plasma levels of TNFα in ob/ob mice

We next tested the potential beneficial effects of BP-**2** on the inflammatory state in *ob/ob* mice. As BP-**2** impaired mononuclear cell arrest in vitro, we investigated its impact on circulating T-lymphocyte and monocyte subpopulations. No significant differences were found in the activation state (CD69 or CD11b expression) of the leukocyte subpopulations in BP-**2**-treated mice (Fig. 5A–C). Additionally, whereas BP-2 treatment significantly lowered the plasma levels of TNFα at 30 mg/kg/d (Fig. 5D), it had no effect on MCP-1/CCL2 or fractalkine/CX_3CL1 plasma levels (Fig. 5E and F).

3.9. BP-2 suppresses T-lymphocyte and macrophage infiltration in the visceral white adipose tissue of ob/ob mice and improves the inflammatory status

Because excess visceral WAT is a known potential independent risk factor for the development of metabolic disorders [37,38], we investigated the effects of BP-**2** on the inflammatory state in the visceral WAT of *ob/ob* mice. BP-**2** treatment significantly suppressed the infiltration of T-lymphocytes (Fig. 6A and B) and macrophages (Fig. 6C and D) at both tested doses.

In agreement with these observations, RNA analysis of visceral WAT showed that BP-**2** treatment significantly decreased the mRNA expression of the proinflammatory cytokine TNFα (Fig. 6E), as well as of the chemokines MCP-1/CCL2 (Fig. 6F) and fractalkine/CX_3CL1 (Fig. 6G). Of note, the mRNA expression of CD206, a known marker of anti-inflammatory M2-like macrophages [39], was significantly increased in visceral WAT at the BP-2 dose of 30 mg/kg/d (Fig. 6H).

Table 2
Biometric and biochemical parameters in *ob/ob* mice treated with BP-2 or vehicle.

	Vehicle	BP-**2** (10 mg/kg/d)	BP-**2** (30 mg/kg/d)
Body-weight gain (g)	3.89 ± 1.16	5.30 ± 0.44	3.97 ± 0.32
Food intake (g)	68.27 ± 2.79	70.47 ± 2.17	67.64 ± 2.21
Glycemia (mg/L)	2482.86 ± 342.68	1310.00 ± 164.09 *	1405.00 ± 93.91 *
Insulin (ng/mL)	1.42 ± 0.65	2.37 ± 0.54	3.12 ± 0.95
HOMA-IR index	25.71 ± 11.68	22.79 ± 5.90	34.78 ± 9.37
Adiponectin (μg/mL)	5.33 ± 0.38	5.81 ± 0.35	5.29 ± 0.28
Total cholesterol (mg/L)	1930.08 ± 158.37	2203.19 ± 184.23	2524.91 ± 390.50
HDL-c (mg/L)	913.05 ± 101.69	755.19 ± 122.00	842.45 ± 185.32
Non-HDL-c (mg/L)	1591.57 ± 509.26	1393.85 ± 160.86	1894.07 ± 350.48
Triglycerides (mg/L)	1777.89 ± 361.91	592.05 ± 86.43 *	517.49 ± 53.24 *
FFA (nmol/μL)	0.56 ± 0.13	0.52 ± 0.10	0.56 ± 0.04
ALT activity (nmol/min/mL)	592.40 ± 83.63	332.70 ± 34.40 *	323.90 ± 36.00 *
AST activity (nmol/min/mL)	11,472.27 ± 1251.06	6450.91 ± 1075.45 *	4751.00 ± 987.28 *

Note. Parameters were measured after a fifteen-days treatment by oral gavage in 6-h fasted mice. HOMA-IR index =[fasting glucose (mmol/L) × fasting insulin (mU/mL)]/22.5). Non-HDL-c (mg/L) = Total cholesterol (mg/L) – HDL-c (mg/L). Data are presented as mean ± SEM of 5–7 independent experiments. * $P < 0.05$ relative to the vehicle-administered control group. Abbreviations: ALT = Alanine Aminotransferase; AST = Aspartate Aminotransferase; FFA = Free Fatty Acids; HDL-c = High-Density Lipoprotein Cholesterol.

3.10. BP-2 suppresses T-lymphocyte and macrophage infiltration and improves inflammation in the liver, but does not alter hepatic triglyceride content

Similar to our findings in visceral WAT, BP-**2** treatment of *ob/ob* mice significantly suppressed T-lymphocyte and macrophage hepatic infiltration at 30 mg/kg/d (Fig. 7A–D). Also, significant decreases in hepatic TNFα and MCP-1/CCL2 mRNA expression were detected in BP-2-treated mice at 30 mg/kg/d (Fig. 7E and F); however, no changes were observed for fractalkine/CX_3CL1 mRNA expression (Fig. 7G). Notably the mRNA expression of CD206 in the liver of *ob/ob* mice was again increased after BP-2 administration (Fig. 7H). In addition, whereas the circulating levels of triglycerides were lower in BP-2-treated *ob/ob* mice than in control *ob/ob* mice, no differences were found in hepatic triglyceride content (Fig. 7I). Nevertheless, BP-**2** treatment was found to modulate relevant PPAR-related target genes associated with lipid metabolism. Particularly, the administration of BP-**2** in *ob/ob* mice at 30 mg/kg/d upregulated the hepatic expression of the gene encoding for carnitine palmitoyltransferase-1A (*Cpt1a*, Fig. S7A), an enzyme involved in FA oxidation, and downregulated the hepatic expression of the gene encoding for apolipoprotein CIII (*Apoc3*, Fig. S7C), a protein that inhibits lipoprotein lipase activity. In contrast, no significant differences were encountered in the mRNA expression of the gene encoding for pyruvate dehydrogenase kinase 4, (*Pdk4,* Fig. S7B), a target gene for PPARγ [40], probably due to the weak agonism displayed by BP-**2** on this nuclear receptor.

4. Discussion

The past few years has witnessed increasing interest in the development of dual/pan-PPAR agonists as drug candidates to regulate both lipid and glucose homeostasis in T2D and MetS, in particular those showing partial PPARγ activation, which is associated with fewer adverse effects [10–12]. Along this line, we recently described a potent dual-PPARα/γ agonist, the natural prenylated benzopyran polycerasoidol (BP-**1**) [16]**.** This natural product shows low cytotoxicity and exerts anti-inflammatory activity through the inhibition of TNFα-induced mononuclear cell-endothelial cell interactions [16]. In an attempt to develop safer and more effective dual/pan-PPAR agonists, and based on polycerasoidol molecular modeling studies [16], here we designed and synthesized the new prenylated benzopyran—2-(ethyl 4'-methyl-heptenoate)− 6-(p-fluorobenzyloxy)− 2-(methyl)-benzodihydropyran (BP-**2**)—using a bioisoster approach. BP-**2** shares structural features with BP-**1** including the benzopyran nucleus linked to a short side-prenylated chain, and key groups that function as anchoring points to the binding domain of PPARα, PPARβ/δ and PPARγ such as the oxygen atom at C-6 position and an ester group. Transactivation assays revealed that BP-**2** activated hPPARα with high efficacy, and also moderately and weakly activated hPPARβ/δ and hPPARγ, respectively, in comparison with their respective reference drugs. Accordingly, BP-**2** might display lower PPARγ-associated adverse effects than those of dual-PPARα/γ agonists with full PPARγ activation. Indeed, BP-**2** had no significant cytotoxic effect on human neutrophils or on primary cultures of human endothelial cells at concentrations up to 77-, 58- or 40-fold higher than its EC_{50} for PPARα, PPARβ/δ or PPARγ agonism, respectively. This indicates that the modifications introduced in the BP-**1** structure to obtain BP-**2** did not result in enhanced toxicity.

Molecular modeling studies revealed that BP-**2** displayed its pharmacophoric portions for PPARα in a closely related spatial form to that reported for BP-**1** [16] and WY-14,643. These studies confirmed that Ser280 forms hydrogen bonds with O1 and with the O atom at C-6, which establishes BP-**2**/PPARα complex formation. Furthermore, the most hydrophobic portion of BP-**2** is located in the same hydrophobic portion (Ile317, Leu460, Ile354, and Met355) as for WY-14,643 and BP-**1** [16], adopting similar spatial arrangements. Interactions of BP-**2** with PPARβ/δ indicate that it spatially locates in the same site as GW501516. MD simulations showed that the A ring, which is located in the hydrophobic pocket formed by the residues of Val245, Val305 Val312, leu219 and Ile213, exhibits strong pi-stacking interactions with Trp228. Additional relevant interactions for complex stabilization were those of the O atom at C-6 with Cys249 and the carbonyl O atom with His413. The analysis per residue showed that GW501516 has stronger interactions with PPARβ/δ than BP-**2**, which is consistent with the PARβ/δ activation assays showing that GW501516 behaves as a stronger ligand than BP-**2**. In regard to PPARγ, simulations revealed that the most relevant amino acids for interactions between BP-**2** and PPARγ binding domains were His449 and Tyr473, which interacted with the carboxyl of the ester group in the prenylated chain and likely act as an anchoring point. In addition, the involvement of Arg280, Ile281, Gly284, Cys285, Leu330, and Ile341 were also identified. Free energy decomposition analysis showed the strongest interactions displayed by rosiglitazone with Tyr473, Phe363 and Met364 (Fig. S3C), which could strengthen PPARγ activity in accordance with the PPAR transactivation assays.

PPAR ligands are powerful therapeutic tools in the control of different metabolic disorders [8,9], which are a clear risk for atherosclerosis development and subsequent cardiovascular events [41]. In addition, it is widely acknowledged that T2D or alterations in lipid metabolism are linked to endothelial dysfunction [8,41,42], a proinflammatory and prothrombotic phenotype of the endothelium [43]. We show that BP-**2** inhibits mononuclear cell arrest to the dysfunctional (TNFα-stimulated) endothelium in a concentration-dependent manner without affecting neutrophil-endothelial cell interactions, suggesting that BP-**2** might prevent atherosclerosis progression without compromising the innate host defense of neutrophils.

CAMs such as ICAM-1 or VCAM-1, as well as the chemokines fractalkine/CX_3CL1 and MCP-1/CCL2, are linked to mononuclear cell arrest [44]. BP-**2** significantly reduced TNFα-induced ICAM-1, VCAM-1 and transmembrane fractalkine/CX_3CL1 endothelial expression and soluble fractalkine/CX_3CL1 release. In this line, MAPK signaling pathways can additionally be modulated by PPAR ligands [4]. In turn, the activation of different components of the MAPK family is associated with NF-κB transactivation [33], which ultimately activates the transcription of

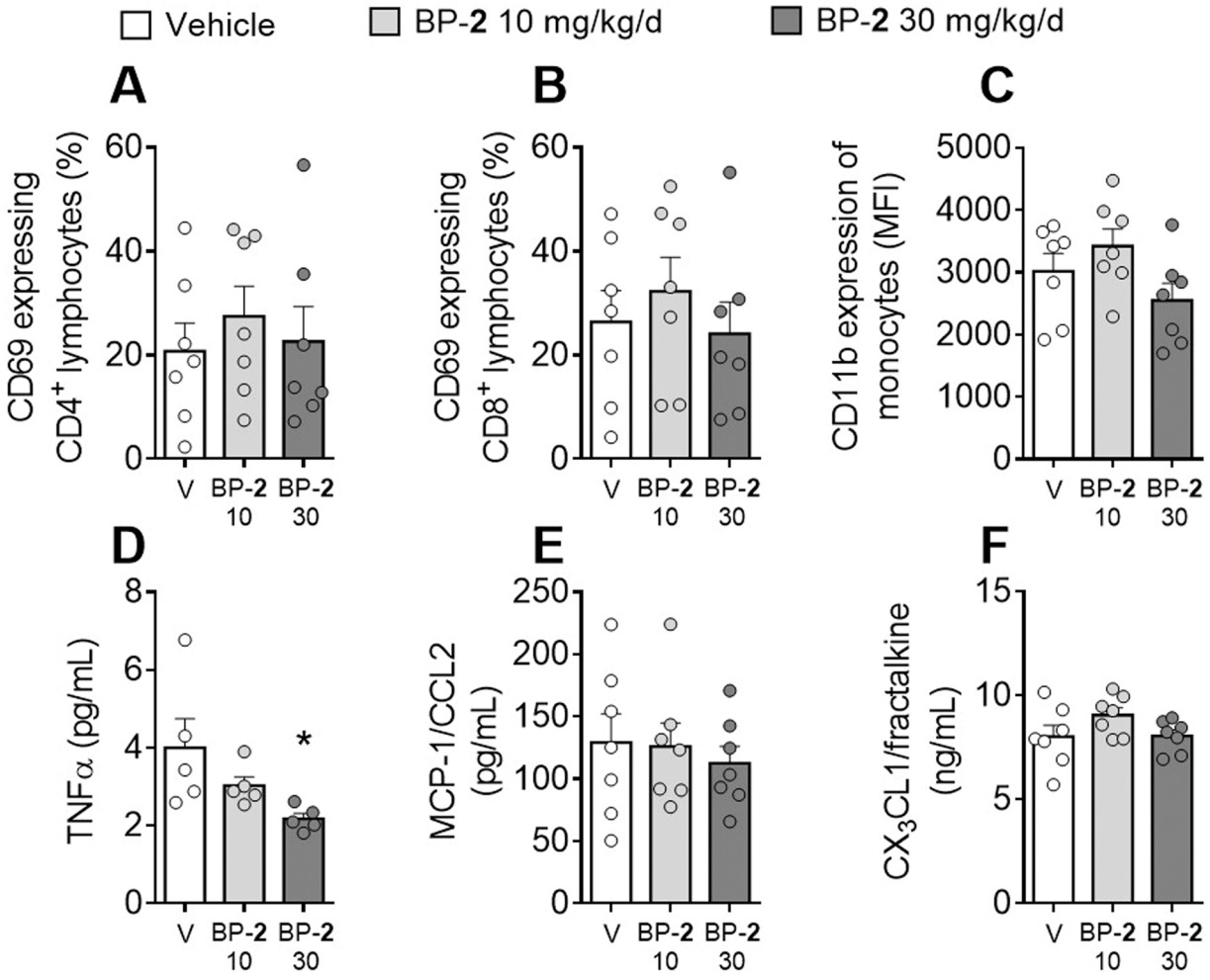

Fig. 5. BP-2 reduces the plasma levels of TNFα in *ob/ob* mice. *Ob/ob* mice were daily treated with compound BP-2 (10 or 30 mg/kg, orally) for 15 days. Flow cytometry analysis of heparinized whole blood co-stained with specific markers for $CD4^+$ lymphocytes (A), $CD8^+$ lymphocytes (B) and monocytes (C), as well as for CD69 (A and B) or CD11b integrin (C). Results are expressed as percentage of positive cells or mean fluorescence intensity (MFI). TNFα (D), MCP-1/CCL2 (E), or soluble CX_3CL1/fractalkine (F) plasma levels (pg/mL or ng/mL) were measured by ELISA. Values are presented as mean ± SEM of 5–7 independent experiments. * $P < 0.05$ relative to vehicle-treated mice.

genes that encode endothelial CAMs and chemokines [34]. In this regard, BP-**2** inhibited both p38-MAPK and NF-κB activation induced by TNFα.

A deeper analysis using RNA silencing suggested that the inhibitory effect of BP-**2** on mononuclear cell-endothelium interactions partly required RXRα/PPARβ/δ interactions, as RXRα- or PPARβ/δ-silencing reversed the inhibitory effect of BP-**2** on mononuclear leukocyte arrest to dysfunctional endothelium. These findings are in agreement with previous reports from our group and others [15,45,46]. As described for BP-**1** [16], RXRα/PPARα interactions were not involved in the inhibitory effect of BP-**2** on this parameter.

PPARα agonists are clinically used in the treatment of hypertriglyceridemia and other dyslipidemias associated with elevated levels of triglycerides [8]. Our findings of a 15-day treatment study of BP-**2** in *ob/ob* mice, an animal model of dyslipidemia and T2D, showed that while the drug had no effect on total cholesterol, HDL-c or LDL-c levels, it reduced circulating triglyceride levels, likely through its PPARα and PPARβ/δ agonism and the subsequent modulation of PPAR-related target genes [47]. No PPARβ/δ agonists are currently approved for clinical use; however, some potential candidates are under clinical trials for T2D and dyslipidemic disorders since PPARβ/δ activation modulates glucose and lipid homeostasis [4,48]. Additionally, selective PPARγ agonists such as TZD, although potent insulin sensitizers and effective drugs for T2D treatment, result in several adverse effects that limits their use [4]. In contrast to TZD, BP-**2** increased neither body weight nor liver triglyceride content [49], but it did improve glycemia without affecting the HOMA-IR index, insulin and adiponectin levels. While PPARγ activation has been widely described to improve insulin sensitivity, in humans and mice, through the up-regulation of adiponectin which results in an insulin level decrease [4,50,51], selective PPARβ/δ activation has been associated to hypoglycemic effects without affecting significantly insulin levels [4,52,53]. Therefore, our results suggest that BP-**2** through PPARβ/δ activation, caused the observed hypoglicemic effects. Furthermore, as hepatotoxicity has been identified as a side effect of some TZDs [8], it is encouraging that BP-**2**-treatment decreased ALT and AST levels, both recognized as markers of hepatic dysfunction.

It is now recognized that, in addition to its energy storage functions, adipose tissue is also an endocrine organ that produces and secretes several mediators that affect insulin sensitivity and systemic inflammation. Both WAT and liver inflammation have been associated with the accumulation of proinflammatory macrophages and T-lymphocytes [54,55]. We found a decrease in the number of macrophages and T-lymphocytes in the WAT and liver of *ob/ob* mice after 15 days treatment with BP-**2**, indicating an improvement in the inflammatory state. Likewise, tissue mRNA expression of relevant cytokines and chemokines were diminished in BP-**2**-treated animals. TNFα is a key cytokine in metabolic disorders and cardiovascular complications [56], and the reduction of its plasma levels and mRNA expression in WAT and liver of

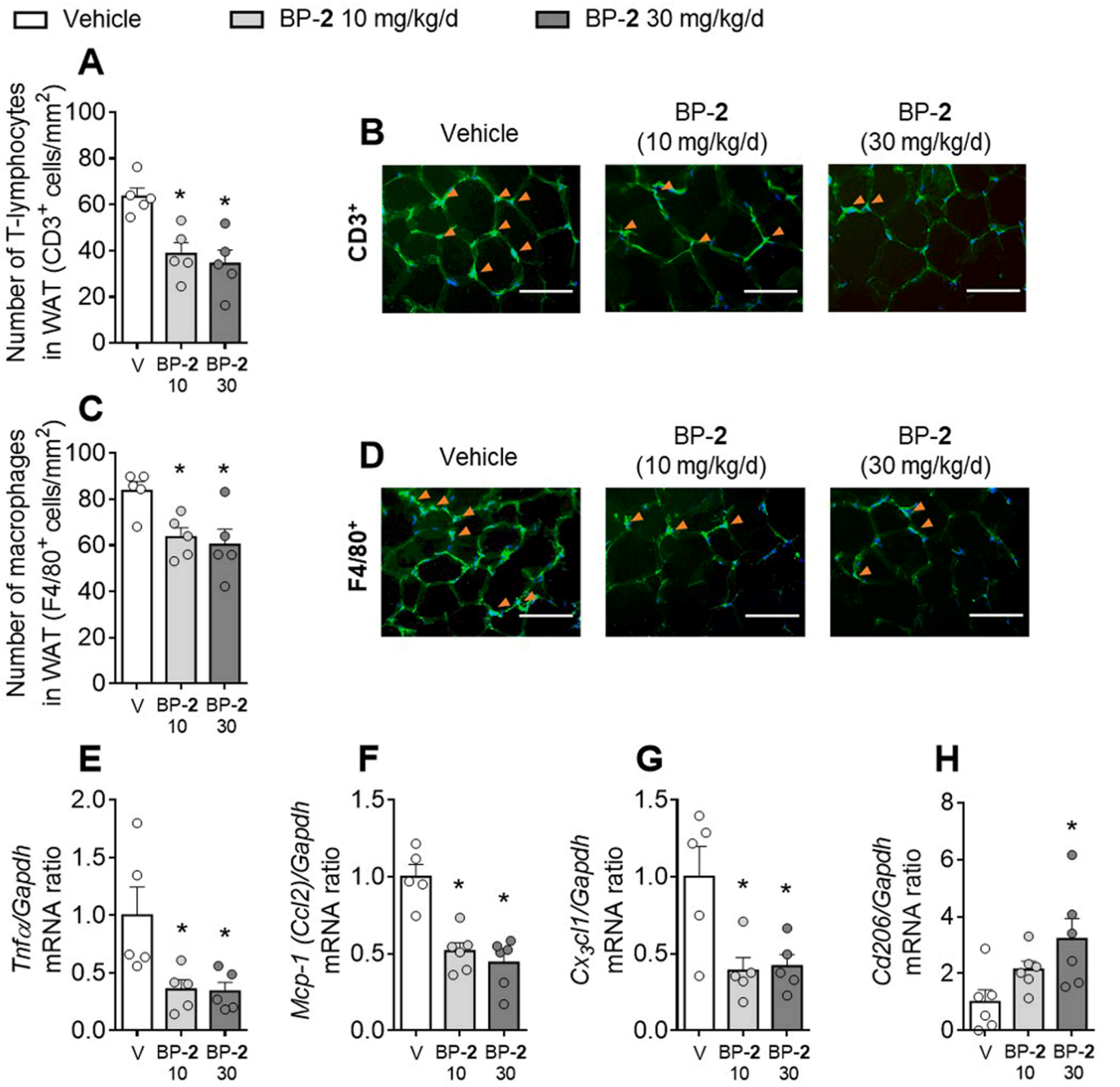

Fig. 6. BP-2 suppresses the infiltration of T-lymphocytes and macrophages and the mRNA expression of *Tnfα*, *Mcp-1/Ccl2* and *Cx$_3$cl1* in WAT of *ob/ob* mice, and increases the mRNA expression of *Cd206*. *Ob/ob* mice were daily treated with compound BP-2 (10 or 30 mg/kg, orally) for 15 days, then WAT was dissected for histological examination and RNA extraction. Quantification of $CD3^+$ (A and B) or $F4/80^+$ cells (C and D) per mm^2 of WAT cross sections by immunofluorescent labeling. Immunoreactivity was visualized using Alexa-fluor 488 secondary antibodies (green) and nuclei were stained with Hoechst dye (blue). Scale bar = 100 μm. mRNA expression of *Tnfα* (E), *Mcp-1/Ccl2* (F), *Cx$_3$cl1* (G) and *Cd206* (H) relative to *Gapdh* in WAT was analyzed by RT-PCR. Values are presented as mean ± SEM of 5–7 independent experiments. * $P < 0.05$ relative to vehicle-treated mice.

BP-**2**-treated *ob/ob* mice highlights the tempering effect of this pan-PPAR agonist on the proinflammatory state associated with different metabolic disorders. Interestingly, the decrease of MCP-1/CCL2 and the increase of CD206 mRNA expression in WAT and liver exerted by BP-**2** administration suggests the polarization of macrophages from a proinflammatory M1-like phenotype to an anti-inflammatory M2-like phenotype, which has been associated with both PPARβ/δ and PPARγ activation [47,57]. Of note, M2-like macrophages might regulate systemic glucose metabolism [39] and protect against hepatic fibrosis [58].

In conclusion, we have designed, synthesized and pharmacologically evaluated in vitro and in vivo a new prenylated benzopyran—BP-**2**—a structural analog of the dual PPARα/γ agonist polycerasoidol BP-**1** [16]. BP-**2** displays pan-PPAR agonism with a strong PPARα-, moderate PPARβ/δ- and weak PPARγ-activity, which should minimize any PPARγ-related adverse effects. BP-**2** exerted anti-inflammatory effects in vitro, inhibiting the adhesion of mononuclear cells to the dysfunctional endothelium through decreased CAM and fractalkine/CX_3CL1 expression via p38MAPK/NFκB activation and RXRα/PPARβ/δ interactions. In vivo, T-lymphocyte and macrophage infiltration into adipose tissue and

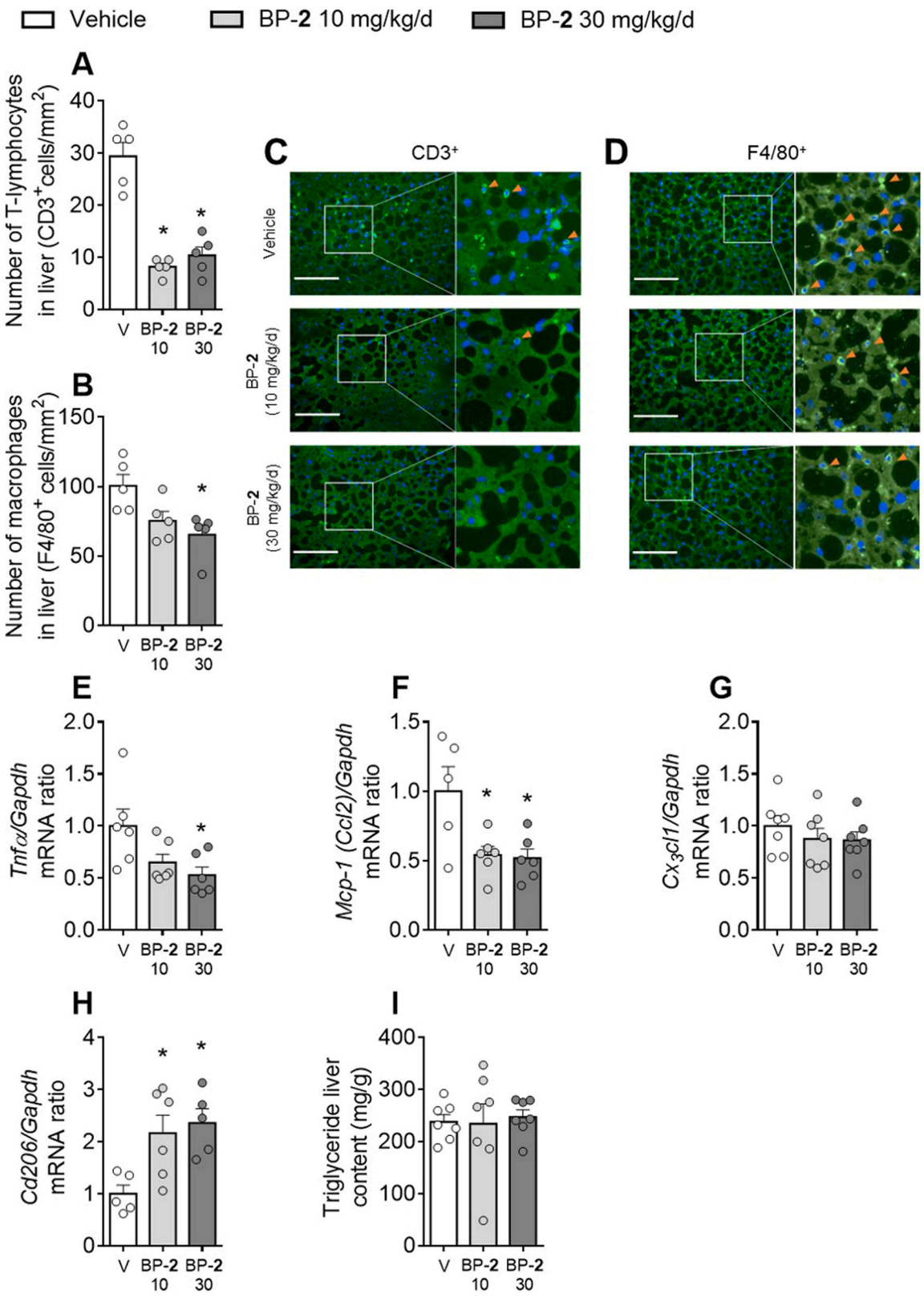

Fig. 7. BP-2 suppresses the infiltration of T-lymphocytes and macrophages and the mRNA expression of *Tnfα* and *Mcp-1/Ccl2* in liver of *ob/ob* mice, and increases the mRNA expression of *Cd206*. *Ob/ob* mice were daily treated with compound BP-2 (10 or 30 mg/kg, po) for 15 days, then the liver was dissected for histological examination, RNA and protein extraction and triglyceride content determination. Quantification of $CD3^+$ (A and C) or $F4/80^+$ cells (B and D) per mm^2 of liver cross sections by immunofluorescent labeling. Immunoreactivity was visualized using Alexa-fluor 488 secondary antibodies (green) and nuclei were stained with Hoechst dye (blue). Scale bar = 100 μm. mRNA expression of *Tnfα* (E), *Mcp-1/Ccl2* (F), *Cx_3cl1* (G) and *Cd206* (H) relative to *Gapdh* in liver was analyzed by RT-PCR. Hepatic triglyceride content (I, mg/g) was determined by enzymatic measurement of glycerol content. Values are presented as mean ± SEM of 5–7 independent experiments. * $P < 0.05$ relative to vehicle-treated mice.

liver of ob/ob mice was markedly reduced and macrophage polarization to an anti-inflammatory M2-like phenotype was observed. Finally, these effects were accompanied by improvements in glycemia and circulating triglyceride levels, key features in reversing MetS. Based on its pan-PPAR activity, our study suggest that BP-**2** is a new lead compound for the treatment of metabolic disorders including atherogenic dyslipidemia and cardiovascular disease.

Funding

This work was supported by the Spanish Ministry of Science and Innovation: [grant numbers SAF2017-89714-R, PID2020-120336RB-I00]; the Carlos III Health Institute (ISCIII) and the European Regional Development Fund (FEDER) [grant numbers PI18/01450, PI18/00209, PI21/02045, PI21-00220]; the Generalitat Valenciana [grant numbers CDEI-04/20A, AICO/2019/250, AICO/2021/081, APOTIP/2020/011, PROMETEO/2019/032]; the Agence Nationale pour la Recherche [grant number ANR-10 LABX-0046]; and the European Research Council [grant number 694717]. Nuria Cabedo was funded by the ISCIII Miguel Servet programme [CP15/00150 and CPII20/00010], co-funded by the European Social Fund. Patrice Marques, Carlos Villarroel-Vicente and Aida Collado were funded by pre-doctoral grants from the Spanish Ministry of Science and Innovation, the ISCIII (PFIS-FI19/00153) and the Generalitat Valenciana, respectively.

CRediT authorship contribution statement

DC, MJS and NC contributed to the conception and design of the study; PM, CV, AC, AG, LV, NH, FG, RDE, CD, LP, DC, MJS and NC acquired, analyzed and interpreted the data; PM, CV, DC, MJS and NC wrote the manuscript and AC, AG, LV, NH, FG, RDE, CD and LP revised it critically. All the authors have read and approved the submission of the manuscript.

Declaration of Competing Interest

No potential conflicts of interest relevant to this article were reported.

Data availability

Data will be made available on request.

Appendix A. Supplementary material

Supplementary data associated with this article can be found in the online version at doi:10.1016/j.phrs.2022.106638.

References

[1] R.H. Eckel, K.G. Alberti, S.M. Grundy, P.Z. Zimmet, The metabolic syndrome, Lancet 375 (9710) (2010) 181–183, https://doi.org/10.1016/s0140-6736(09)61794-3.

[2] P. Marques, A. Collado, S. Martinez-Hervás, E. Domingo, E. Benito, L. Piqueras, et al., Systemic inflammation in metabolic syndrome: increased platelet and leukocyte activation, and key role of CX(3)CL1/CX(3)CR1 and CCL2/CCR2 axes in arterial platelet-proinflammatory monocyte adhesion, J. Clin. Med. 8 (5) (2019) 708, https://doi.org/10.3390/jcm8050708.

[3] V. Dubois, J. Eeckhoute, P. Lefebvre, B. Staels, Distinct but complementary contributions of PPAR isotypes to energy homeostasis, J. Clin. Investig. 127 (4) (2017) 1202–1214, https://doi.org/10.1172/JCI88894.

[4] C. Villarroel-Vicente, S. Gutiérrez-Palomo, J. Ferri, D. Cortes, N. Cabedo, Natural products and analogs as preventive agents for metabolic syndrome via peroxisome proliferator-activated receptors: an overview, Eur. J. Med. Chem. 221 (2021), 113535, https://doi.org/10.1016/j.ejmech.2021.113535.

[5] L. Piqueras, A.R. Reynolds, K.M. Hodivala-Dilke, A. Alfranca, J.M. Redondo, T. Hatae, et al., Activation of PPARbeta/delta induces endothelial cell proliferation and angiogenesis, Arterioscler. Thromb. Vasc. Biol. 27 (1) (2007) 63–69, https://doi.org/10.1161/01.Atv.0000250972.83623.61.

[6] W. Wahli, L. Michalik, PPARs at the crossroads of lipid signaling and inflammation, Trends Endocrinol. Metab. 23 (7) (2012) 351–363, https://doi.org/10.1016/j.tem.2012.05.001.

[7] L.A. Moraes, L. Piqueras, D. Bishop-Bailey, Peroxisome proliferator-activated receptors and inflammation, Pharmacol. Ther. 110 (3) (2006) 371–385, https://doi.org/10.1016/j.pharmthera.2005.08.007.

[8] W.S. Cheang, X.Y. Tian, W.T. Wong, Y. Huang, The peroxisome proliferator-activated receptors in cardiovascular diseases: experimental benefits and clinical challenges, Br. J. Pharmacol. 172 (23) (2015) 5512–5522, https://doi.org/10.1111/bph.13029.

[9] R.S. Rosenson, R.S. Wright, M. Farkouh, J. Plutzky, Modulating peroxisome proliferator-activated receptors for therapeutic benefit? Biology, clinical experience, and future prospects, Am. Heart J. 164 (5) (2012) 672–680, https://doi.org/10.1016/j.ahj.2012.06.023.

[10] M.B. Wright, M. Bortolini, M. Tadayyon, M. Bopst, Minireview: challenges and opportunities in development of PPAR agonists, Mol. Endocrinol. 28 (11) (2014) 1756–1768, https://doi.org/10.1210/me.2013-1427.

[11] F.L. Dunn, L.S. Higgins, J. Fredrickson, A.M. DePaoli, Selective modulation of PPARγ activity can lower plasma glucose without typical thiazolidinedione side-effects in patients with Type 2 diabetes, J. Diabetes Complicat. 25 (3) (2011) 151–158, https://doi.org/10.1016/j.jdiacomp.2010.06.006.

[12] L.S. Higgins, A.M. Depaoli, Selective peroxisome proliferator-activated receptor gamma (PPARgamma) modulation as a strategy for safer therapeutic PPARgamma activation, Am. J. Clin. Nutr. 91 (1) (2010) 267s–272ss, https://doi.org/10.3945/ajcn.2009.28449E.

[13] M.Y. Lee, R. Choi, H.M. Kim, E.J. Cho, B.H. Kim, Y.S. Choi, et al., Peroxisome proliferator-activated receptor δ agonist attenuates hepatic steatosis by anti-inflammatory mechanism, Exp. Mol. Med. 44 (10) (2012) 578–585, https://doi.org/10.3858/emm.2012.44.10.066.

[14] X. Palomer, E. Barroso, J. Pizarro-Delgado, L. Peña, G. Botteri, M. Zarei, et al., PPARβ/δ: a key therapeutic target in metabolic disorders, Int. J. Mol. Sci. 19 (3) (2018) 913, https://doi.org/10.3390/ijms19030913.

[15] L. Piqueras, M.J. Sanz, M. Perretti, E. Morcillo, L. Norling, J.A. Mitchell, et al., Activation of PPARbeta/delta inhibits leukocyte recruitment, cell adhesion molecule expression, and chemokine release, J. Leukoc. Biol. 86 (1) (2009) 115–122, https://doi.org/10.1189/jlb.0508284.

[16] A. Bermejo, A. Collado, I. Barrachina, P. Marqués, N. El Aouad, X. Franck, et al., Polycerasoidol, a natural prenylated benzopyran with a dual PPARα/PPARγ agonist activity and anti-inflammatory effect, J. Nat. Prod. 82 (7) (2019) 1802–1812, https://doi.org/10.1021/acs.jnatprod.9b00003.

[17] T. Mateo, Y. Naim Abu Nabah, M. Losada, R. Estelles, C. Company, B. Bedrina, et al., A critical role for TNFalpha in the selective attachment of mononuclear leukocytes to angiotensin-II-stimulated arterioles, Blood 110 (6) (2007) 1895–1902, https://doi.org/10.1182/blood-2007-01-070607.

[18] E.A. Jaffe, R.L. Nachman, C.G. Becker, C.R. Minick, Culture of human endothelial cells derived from umbilical veins. Identification by morphologic and immunologic criteria, J. Clin. Investig. 52 (11) (1973) 2745–2756, https://doi.org/10.1172/JCI107470.

[19] L.E. Smith, S. Rimmer, S. MacNeil, Examination of the effects of poly(N-vinylpyrrolidinone) hydrogels in direct and indirect contact with cells, Biomaterials 27 (14) (2006) 2806–2812, https://doi.org/10.1016/j.biomaterials.2005.12.018.

[20] M.C. Martin, I. Dransfield, C. Haslett, A.G. Rossi, Cyclic AMP regulation of neutrophil apoptosis occurs via a novel protein kinase A-independent signaling pathway, J. Biol. Chem. 276 (48) (2001) 45041–45050, https://doi.org/10.1074/jbc.M105197200.

[21] M.J. Sanz, F. Albertos, E. Otero, M. Juez, E.J. Morcillo, L. Piqueras, Retinoid X receptor agonists impair arterial mononuclear cell recruitment through peroxisome proliferator-activated receptor-gamma activation, J. Immunol. 189 (1) (2012) 411–424, https://doi.org/10.4049/jimmunol.1102942.

[22] C. Rius, M. Abu-Taha, C. Hermenegildo, L. Piqueras, J.M. Cerda-Nicolas, A. C. Issekutz, et al., Trans- but not cis-resveratrol impairs angiotensin-II-mediated vascular inflammation through inhibition of NF-kappaB activation and peroxisome proliferator-activated receptor-gamma upregulation, J. Immunol. 185 (6) (2010) 3718–3727, https://doi.org/10.4049/jimmunol.1001043.

[23] N. Percie du Sert, V. Hurst, A. Ahluwalia, S. Alam, M.T. Avey, M. Baker, et al., The ARRIVE guidelines 2.0: Updated guidelines for reporting animal research, Br. J. Pharmacol. 177 (16) (2020) 3617–3624, https://doi.org/10.1111/bph.15193.

[24] Q. Ren, L. Deng, Z. Zhou, X. Wang, L. Hu, R. Xie, et al., Design, synthesis, and biological evaluation of novel dual PPARα/δ agonists for the treatment of T2DM, Bioorg. Chem. 101 (2020), 103963, https://doi.org/10.1016/j.bioorg.2020.103963.

[25] Z. Li, Y. Chen, Z. Zhou, L. Deng, Y. Xu, L. Hu, et al., Discovery of first-in-class thiazole-based dual FFA1/PPARδ agonists as potential anti-diabetic agents, Eur. J. Med. Chem. 164 (2019) 352–365, https://doi.org/10.1016/j.ejmech.2018.12.069.

[26] Z. Li, C. Liu, Z. Zhou, L. Hu, L. Deng, Q. Ren, et al., A novel FFA1 agonist, CPU025, improves glucose-lipid metabolism and alleviates fatty liver in obese-diabetic (ob/ob) mice, Pharmacol. Res. 153 (2020), 104679, https://doi.org/10.1016/j.phrs.2020.104679.

[27] E. Blanc-Delmas, N. Lebegue, V. Wallez, V. Leclerc, S. Yous, P. Carato, et al., Novel 1,3-dicarbonyl compounds having 2(3H)-benzazolonic heterocycles as PPARgamma agonists, Bioorg. Med. Chem. 14 (22) (2006) 7377–7391, https://doi.org/10.1016/j.bmc.2006.07.029.

[28] D.K. Zaafar, S.A. Zaitone, Y.M. Moustafa, Role of metformin in suppressing 1,2-dimethylhydrazine-induced colon cancer in diabetic and non-diabetic mice: effect

on tumor angiogenesis and cell proliferation, PLoS One 9 (6) (2014), e100562, https://doi.org/10.1371/journal.pone.0100562.
[29] I. Andrés-Blasco, A. Herrero-Cervera, Á. Vinué, S. Martínez-Hervás, L. Piqueras, M. J. Sanz, et al., Hepatic lipase deficiency produces glucose intolerance, inflammation and hepatic steatosis, J. Endocrinol. 227 (3) (2015) 179–191, https://doi.org/10.1530/joe-15-0219.
[30] N. Kuwabara, T. Oyama, D. Tomioka, M. Ohashi, J. Yanagisawa, T. Shimizu, et al., Peroxisome proliferator-activated receptors (PPARs) have multiple binding points that accommodate ligands in various conformations: phenylpropanoic acid-type PPAR ligands bind to PPAR in different conformations, depending on the subtype, J. Med. Chem. 55 (2) (2012) 893–902, https://doi.org/10.1021/jm2014293.
[31] C.C. Wu, T.J. Baiga, M. Downes, J.J. La Clair, A.R. Atkins, S.B. Richard, et al., Structural basis for specific ligation of the peroxisome proliferator-activated receptor δ, Proc. Natl. Acad. Sci. USA 114 (13) (2017) E2563–e70, https://doi.org/10.1073/pnas.1621513114.
[32] M. Jiao, F. Ren, L. Zhou, X. Zhang, L. Zhang, T. Wen, et al., Peroxisome proliferator-activated receptor α activation attenuates the inflammatory response to protect the liver from acute failure by promoting the autophagy pathway, Cell Death Dis. 5 (8) (2014), e1397, https://doi.org/10.1038/cddis.2014.361.
[33] W. Vanden Berghe, S. Plaisance, E. Boone, K. De Bosscher, M.L. Schmitz, W. Fiers, et al., p38 and extracellular signal-regulated kinase mitogen-activated protein kinase pathways are required for nuclear factor-kappaB p65 transactivation mediated by tumor necrosis factor, J. Biol. Chem. 273 (6) (1998) 3285–3290, https://doi.org/10.1074/jbc.273.6.3285.
[34] C. Monaco, E. Paleolog, Nuclear factor kappaB: a potential therapeutic target in atherosclerosis and thrombosis, Cardiovasc Res. 61 (4) (2004) 671–682, https://doi.org/10.1016/j.cardiores.2003.11.038.
[35] M.C. Carmona, K. Louche, M. Nibbelink, B. Prunet, A. Bross, M. Desbazeille, et al., Fenofibrate prevents Rosiglitazone-induced body weight gain in ob/ob mice, Int. J. Obes. 29 (7) (2005) 864–871, https://doi.org/10.1038/sj.ijo.0802943.
[36] H.E. Lebovitz, M. Kreider, M.I. Freed, Evaluation of liver function in type 2 diabetic patients during clinical trials, Diabetes Care 25 (5) (2002) 815, https://doi.org/10.2337/diacare.25.5.815.
[37] R.V. Shah, V.L. Murthy, S.A. Abbasi, R. Blankstein, R.Y. Kwong, A.B. Goldfine, et al., Visceral adiposity and the risk of metabolic syndrome across body mass index: the MESA study, JACC Cardiovasc. Imaging 7 (12) (2014) 1221–1235, https://doi.org/10.1016/j.jcmg.2014.07.017.
[38] T. Karlsson, M. Rask-Andersen, G. Pan, J. Höglund, C. Wadelius, W.E. Ek, et al., Contribution of genetics to visceral adiposity and its relation to cardiovascular and metabolic disease, Nat. Med. 25 (9) (2019) 1390–1395, https://doi.org/10.1038/s41591-019-0563-7.
[39] A. Nawaz, A. Aminuddin, T. Kado, A. Takikawa, S. Yamamoto, K. Tsuneyama, et al., CD206(+) M2-like macrophages regulate systemic glucose metabolism by inhibiting proliferation of adipocyte progenitors, Nat. Commun. 8 (1) (2017) 286, https://doi.org/10.1038/s41467-017-00231-1.
[40] S. Zhang, M.W. Hulver, R.P. McMillan, M.A. Cline, E.R. Gilbert, The pivotal role of pyruvate dehydrogenase kinases in metabolic flexibility, Nutr. Metab. 11 (1) (2014) 10, https://doi.org/10.1186/1743-7075-11-10.
[41] S.M. Grundy, Obesity, metabolic syndrome, and cardiovascular disease, J. Clin. Endocrinol. Metab. 89 (6) (2004) 2595–2600, https://doi.org/10.1210/jc.2004-0372.
[42] H. Zhang, K.C. Dellsperger, C. Zhang, The link between metabolic abnormalities and endothelial dysfunction in type 2 diabetes: an update, Basic Res. Cardiol. 107 (1) (2012) 237, https://doi.org/10.1007/s00395-011-0237-1.
[43] U. Landmesser, B. Hornig, H. Drexler, Endothelial function: a critical determinant in atherosclerosis? Circulation 109 (21 (Suppl. 1)) (2004) Ii27–Ii33, https://doi.org/10.1161/01.CIR.0000129501.88485.1f.
[44] P. Marques, E. Domingo, A. Rubio, S. Martinez-Hervás, J.F. Ascaso, L. Piqueras, et al., Beneficial effects of PCSK9 inhibition with alirocumab in familial hypercholesterolemia involve modulation of new immune players, Biomed. Pharmacother. 145 (2022), 112460, https://doi.org/10.1016/j.biopha.2021.112460.
[45] Y. Fan, Y. Wang, Z. Tang, H. Zhang, X. Qin, Y. Zhu, et al., Suppression of pro-inflammatory adhesion molecules by PPAR-delta in human vascular endothelial cells, Arterioscler. Thromb. Vasc. Biol. 28 (2) (2008) 315–321, https://doi.org/10.1161/atvbaha.107.149815.
[46] A.M. Quintela, R. Jiménez, M. Gómez-Guzmán, M.J. Zarzuelo, P. Galindo, M. Sánchez, et al., Activation of peroxisome proliferator-activated receptor-β/-δ (PPARβ/δ) prevents endothelial dysfunction in type 1 diabetic rats, Free Radic. Biol. Med. 53 (4) (2012) 730–741, https://doi.org/10.1016/j.freeradbiomed.2012.05.045.
[47] S.J. Bensinger, P. Tontonoz, Integration of metabolism and inflammation by lipid-activated nuclear receptors, Nature 454 (7203) (2008) 470–477, https://doi.org/10.1038/nature07202.
[48] A. Gastaldelli, N. Stefan, H.-U. Häring, Liver-targeting drugs and their effect on blood glucose and hepatic lipids, Diabetologia 64 (7) (2021) 1461–1479, https://doi.org/10.1007/s00125-021-05442-2.
[49] Y. Wang, T. Nakajima, F.J. Gonzalez, N. Tanaka, PPARs as metabolic regulators in the liver: lessons from liver-specific PPAR-null mice, Int. J. Mol. Sci. 21 (6) (2020) 2061, https://doi.org/10.3390/ijms21062061.
[50] H.J. Kim, S.K. Kim, W.S. Shim, J.H. Lee, K.Y. Hur, E.S. Kang, et al., Rosiglitazone improves insulin sensitivity with increased serum leptin levels in patients with type 2 diabetes mellitus, Diabetes Res. Clin. Pract. 81 (1) (2008) 42–49, https://doi.org/10.1016/j.diabres.2008.02.001.
[51] J.M. Olefsky, Treatment of insulin resistance with peroxisome proliferator-activated receptor gamma agonists, J. Clin. Investig. 106 (4) (2000) 467–472, https://doi.org/10.1172/jci10843.
[52] C.H. Lee, P. Olson, A. Hevener, I. Mehl, L.W. Chong, J.M. Olefsky, et al., PPARdelta regulates glucose metabolism and insulin sensitivity, Proc. Natl. Acad. Sci. USA 103 (9) (2006) 3444–3449, https://doi.org/10.1073/pnas.0511253103.
[53] D. Aguilar-Recarte, X. Palomer, W. Wahli, M. Vázquez-Carrera, The PPARβ/δ-AMPK connection in the treatment of insulin resistance, Int. J. Mol. Sci. 22 (16) (2021) 8555, https://doi.org/10.3390/ijms22168555.
[54] V.J. Vieira-Potter, Inflammation and macrophage modulation in adipose tissues, Cell Microbiol. 16 (10) (2014) 1484–1492, https://doi.org/10.1111/cmi.12336.
[55] M.W. Robinson, C. Harmon, C. O'Farrelly, Liver immunology and its role in inflammation and homeostasis, Cell Mol. Immunol. 13 (3) (2016) 267–276, https://doi.org/10.1038/cmi.2016.3.
[56] C. Popa, M.G. Netea, P.L. van Riel, J.W. van der Meer, A.F. Stalenhoef, The role of TNF-alpha in chronic inflammatory conditions, intermediary metabolism, and cardiovascular risk, J. Lipid Res. 48 (4) (2007) 751–762, https://doi.org/10.1194/jlr.R600021-JLR200.
[57] S. Francque, G. Szabo, M.F. Abdelmalek, C.D. Byrne, K. Cusi, J.-F. Dufour, et al., Nonalcoholic steatohepatitis: the role of peroxisome proliferator-activated receptors, Nat. Rev. Gastroenterol. Hepatol. 18 (1) (2021) 24–39, https://doi.org/10.1038/s41575-020-00366-5.
[58] L. Bai, X. Liu, Q. Zheng, M. Kong, X. Zhang, R. Hu, et al., M2-like macrophages in the fibrotic liver protect mice against lethal insults through conferring apoptosis resistance to hepatocytes, Sci. Rep. 7 (1) (2017) 10518, https://doi.org/10.1038/s41598-017-11303-z.